Daniele Botto
Costruzione di Motori per Aeromobili
Hertz contacts & bearings - Chapter 3

POLITECNICO DI TORINO

© Prof. M.M. Gola

Chapters

1 Hertz theory and applications

2 Rolling bearings: static loading

3 Rolling bearings: fatigue

Index of contents

Sect. 1 lays the foundations of the sub-surface fatigue in rolling contacts: it shows the stress field inside the bearing ring and how it varies in time when a rolling body moves on the raceway.

Once this part of the problem description is grasped, the reader will be ready to engage, Sect. 2, into the Lundberg-Palmgren[*, **] theory which is the basis for the formulation of a bearing life model.

They supposed that a subsurface crack initiates due to the simultaneous occurrence, at a particular depth, of the maximum orthogonal shear stress and of a weak point in the material. They applied the so called "Weibull weakest link theory".

Since the material microstructure is not explicitly described, the inhomogeneous and random material features are taken into account by assuming that fatigue life follows a Weibull distribution.

[*] Lundberg, G., Palmgren, A., 1947, "Dynamic Capacity of Rolling Bearings," Acta Polytech. Scand., Mech. Eng. Ser., 1(3), pp. 1–52

[**] Lundberg, G., Palmgren, A., 1952, "Dynamic Capacity of Roller Bearings," Acta Polytech. Scand., Mech. Eng. Ser., 2(4), pp. 96–127

Fatigue of bearings The surface failure commonly found in ball or roller bearings, depends on rolling fatigue, a type of contact fatigue. RCF, i.e. **R**olling **C**ontact **F**atigue, is a frequently used acronym.

This type of failure can also be found in gears, cams, valves and rails.

Contact fatigue differs from classic structural fatigue, bending or torsional. In summary, one surface moves over the other in a rolling motion, as in a ball or roller rolling over a raceway.

The contact geometry and the motion of the rolling elements produces an alternating subsurface shear stress. Subsurface plastic strain builds up with increasing cycles until a crack is generated.

The crack then propagates until a pit is formed.

Once surface pitting has initiated, the bearing becomes noisy and rough running.

Then, RCF is a material failure caused by the application of repeated stresses to a small volume of material.

Even when operating correctly, rolling element bearings will eventually fail as a result of a surface fatigue phenomenon.

Rolling element bearing surface fatigue is characterized by pitting and spalling, which liberate particles from the surface of a raceway or of a rolling element in the load zone, and leaves craters that act as stress concentration sites. Subsequent contacts at those sites cause progression of the spalling process.
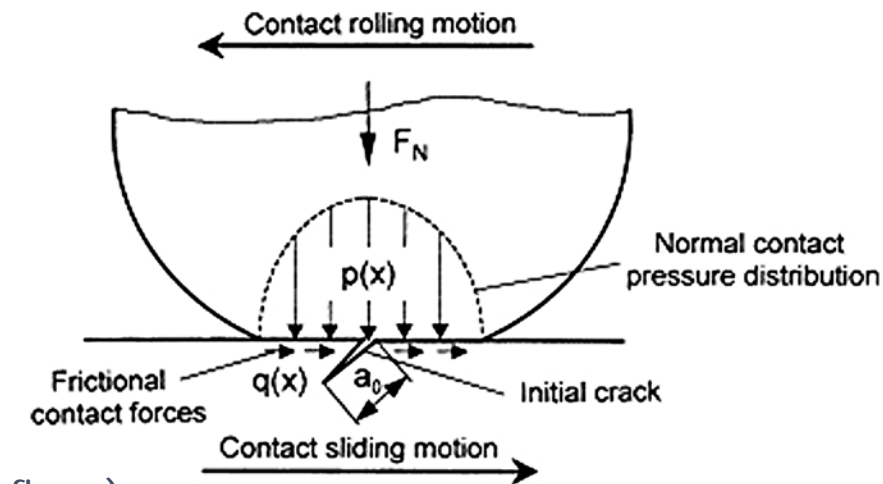
We can today say that the two most dominant RCF mechanisms are subsurface originated spalling and surface originated pitting. These are often competing modes of failure, and the ultimate mechanism that prevails depends on a number of factors, e.g., surface quality, lubricant cleanliness, material quality, etc.

In most of the past literature, spalling and pitting have been used indiscriminately, or were used to designate different severities of surface contact fatigue.

Surface originated **pitting** occurs in cases where surface dents or scratches are present. Here, a crack initiates at the surface stress concentrator and thereafter propagates at a shallow angle (15–30 deg) to the surface (fig. a).

The influence of a lubricating fluid, driven into the crack by hydraulic mechanism, should also be considered.

The crack branches up toward the free surface, removing a piece of surface material and forms a pit.

Pitting appears as shallow craters at contact surfaces with a depth of, at most, the thickness of the work-hardened layer ($\approx$ 10 µm).
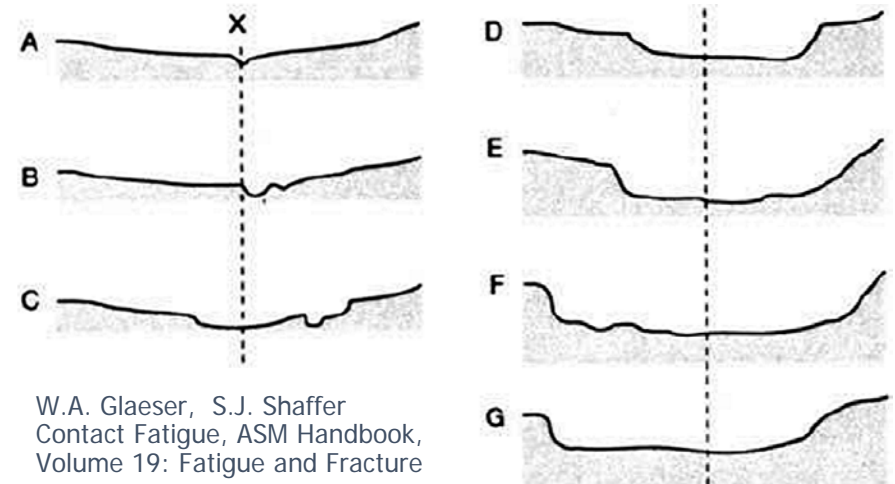

fig. a)

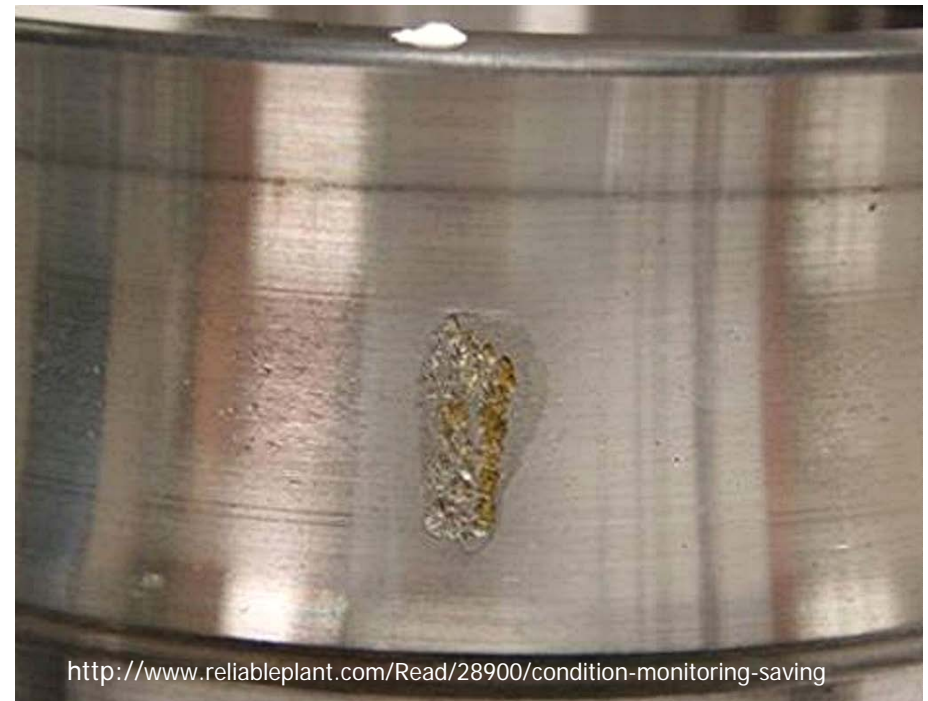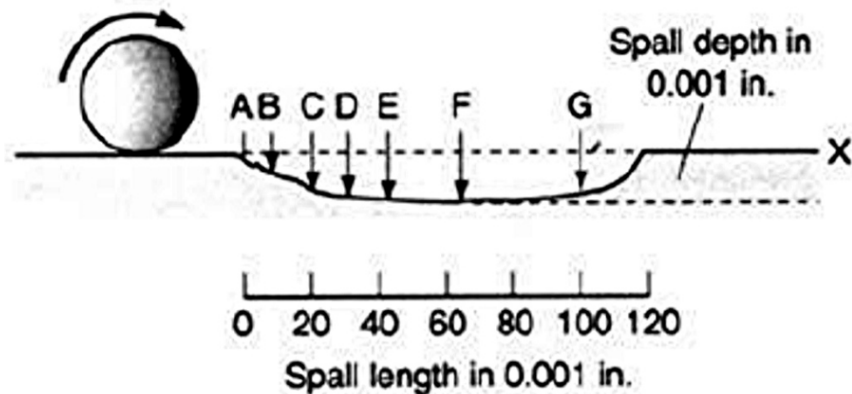Ren Z., Glodez S., Fajdiga G., Ulbin M., Surface initiated crack growth simulation in moving lubricated contact, Theoretical and Applied Fracture Mechanics, Vol. 38, 2, 2002, 141–149

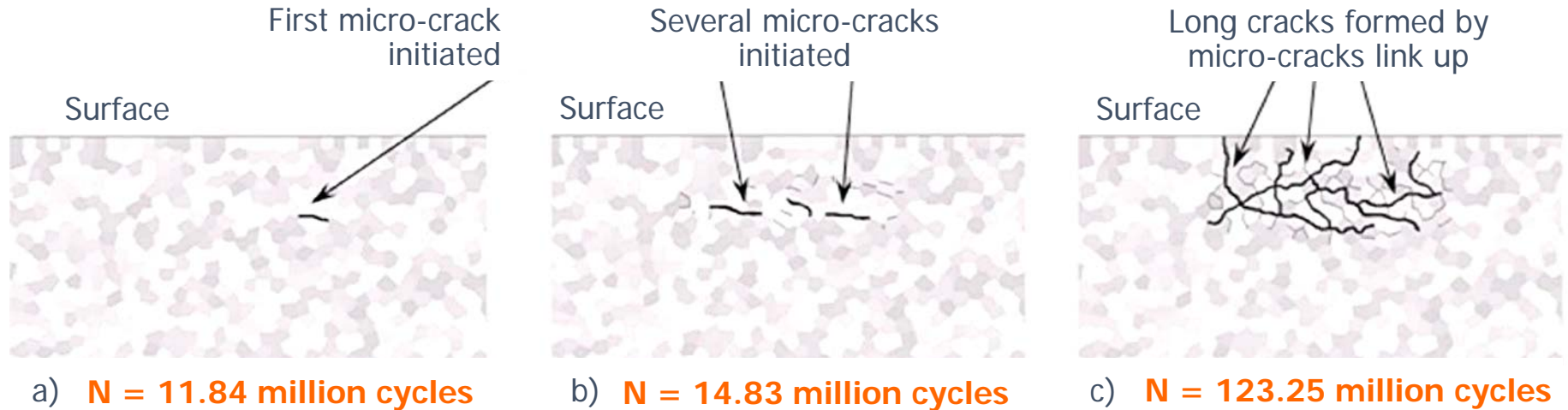http://www.nskamericas.com/cps/rde/xchg/na_en/hs.xsl/pitting.html

Subsurface originated **spalling** occurs when microcracks originate below the surface at material inhomogeneities such as nonmetallic inclusions and propagate toward the surface to form a surface spall.

While pitting is the formation of shallow craters by surface-defect fatigue, spalling is the formation of deeper cavities by subsurface-defect fatigue.

Spalling leaves deeper cavities at contact surfaces with a depth of 20 µm to 100 µm.

http://www.reliableplant.com/Read/28900/condition-monitoring-saving

W.A. Glaeser, S.J. Shaffer
Contact Fatigue, ASM Handbook,
Volume 19: Fatigue and Fracture

First micro-crack initiated

Several micro-cracks initiated

Long cracks formed by micro-cracks link up

Surface

Surface

Surface

a) **N = 11.84 million cycles**   b) **N = 14.83 million cycles**   c) **N = 123.25 million cycles**

Contrary to pitting, spall formation is manifested through several distinct cracks rather than a single crack as assumed in models based on fracture mechanics. The figures above are from a numerical simulation*, which however is confirmed by metallographic observations on spalled sections of contacting elements.   *Sadeghi, F. et al., 2009, "A Review of Rolling Contact Fatigue," ASME Journal of Tribology, Vol. 131(4), 0414031)
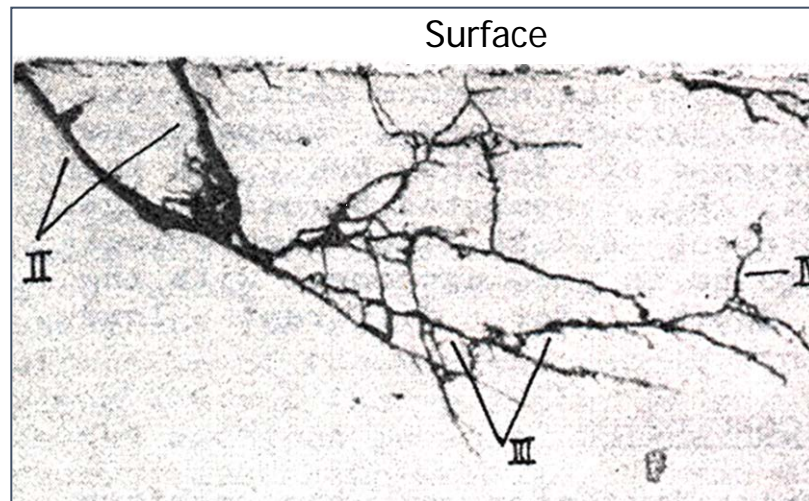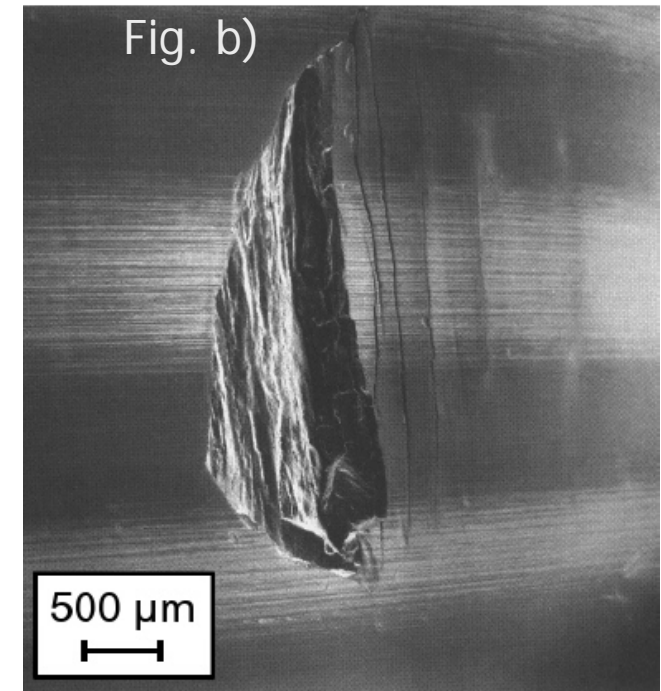
Surface

The micrograph on the left shows how microcracks originate below the surface (at inclusions or other material discontinuities) and propagate toward the surface to form a surface spall.

from Lou, B., Han, L., Lu, Z., Liu, S., and Shen, F., 1990, "The Rolling Contact Fatigue Behaviors in Carburized and Hardened Steel," Fatigue 90: Proceedings of the Fourth International Conference on Fatigue and Fatigue Thresholds, Honolulu, HI, H. Kitagawa and T. Tanaka, eds., pp. 627–632

Fig. a)

surface crack

cracking from sub-surface stresses
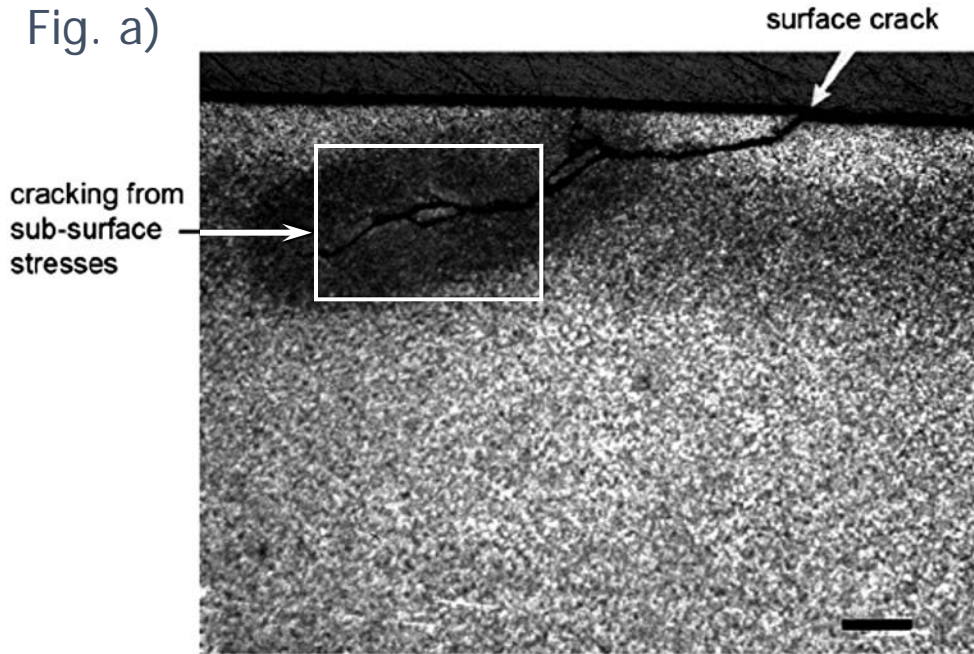
G. E. Dambaugh, Fatigue Considerations of High Strength Rolling Bearing Steels, Schaeffler Group USA, Inc.

Fig. b)

500 μm

W. Nierlich, J. Gegner, Material Response Models for Sub-surface, fnd Surface Rolling Contact Fatigue, Proc. MMT-2006,. 4th Int. Conf. Math. Modeling Computer Simul. Material Technol.

Fig. a) shows, in section, a classical material fatigue cracking typically developed *beneath* the surface of the raceway.

Fig. b) is a SEM micrograph of sub-surface induced spalling on the inner ring raceway, deep grove ball bearing, with crack formation; depth 100 to 300 μm (rolling direction left to right).

There are a number of differences between classical fatigue and RCF that make it impossible to directly apply the results from classical fatigue to RCF. The most important differences can be listed as follows.

1. The state of stress at contacts is complex and <u>multiaxial</u>, governed by the Hertz contact theory. Contrary to most classical fatigue phenomena, rolling contact fatigue is typically a multiaxial fatigue mechanism. A multiaxial fatigue criterion should be applied.

2. Contact fatigue has <u>no endurance limit</u>. If one compares the fatigue lives of cyclic torsion or bending with rolling contact, the latter are seven orders of magnitude greater. Rolling contact life involves tens to hundreds of millions of cycles.

3. There is a <u>high hydrostatic stress</u> component which is absent in classical tension-compression or bending fatigue.

4. Fatigue occurs in a very small volume of stressed material. Typical bearing contact widths are of the order of 200–1000 μm.

5. Contrary to classical fatigue, the loading history at a point below the surface is non-proportional i.e., the stress components do not rise and fall with time in the same proportion to each other (the peaks of the two normal stresses do not coincide with the peaks for the shear stress). There is a complete reversal of the shear stress while the normal stresses always remain compressive.

6. The principal axes in non-conformal contacts constantly change in direction during a stress cycle due to which the planes of maximum shear stress also keep changing. Thus, it is difficult to identify the planes where maximum fatigue damage occurs.

7. A further complication are residual stresses produced when the elastic limit is exceeded in the first application of the load but all further cycles are within the elastic limit (broken lines in slide 13 of this Section).

Quoting from T. A. Harris, R. M. Barnsby, Life ratings for ball and roller bearings, Journal of Engineering Tribology, 2001:

In 1947, Gustav Lundberg and Arvid Palmgren produced what is considered the most significant publication on load and life ratings of rolling bearings. Based on the work of Waloddi Weibull, they postulated that fatigue cracking commences at material weak points below the rolling contact surfaces. The amounts and types of weak points in bearing raceway and rolling element materials are functions of material chemical composition, metallurgical structure and homogeneity. The greater the volume of material stressed, the greater also, according to Weibull, is the risk of fatigue failure. In 1949, Weibull published a specific work on his statistical theory for fatigue failure in solids.

Based on the Weibull theory, Lundberg and Palmgren developed the equations which underpin all their subsequent developments, illustrated in Sect. 2 of this Chapter.
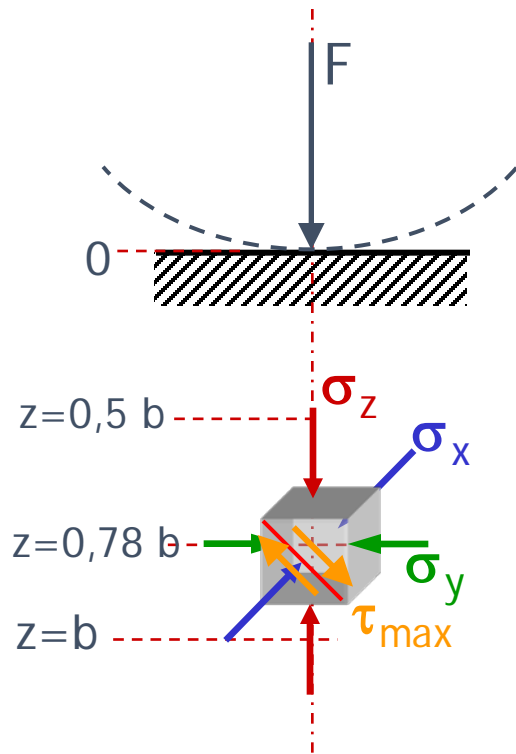
It has been generally found in the study of ductile metal yield that deviatoric components of the stress tensor are responsible for the onset of metal plasticity, not the hydrostatic stress components.

Fatigue is generated in an area of a mechanical member that sees plasticity, or the development of *slip-bands* under cyclic loading.

We know (Ch.1, Sect. 8. sl. 3) that for instance with cylindrical rollers that maximum shear stress τ_{max} occurs at a depth of ~0,78 b and amounts to ~0,3 p_{max}; $\sigma_{eq} = 2 \cdot \tau_{max} = 0,6\ p_{max}$, with Von Mises stress very near to that value.

This stress varies from zero to a maximum when a ball or a roller approaches the vertical on the element, then it vanishes to zero as it moves away.

Then it might be considered responsible of fatigue.
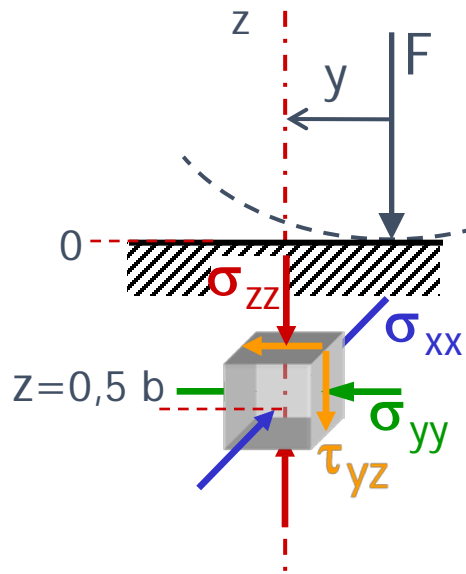
However, fatigue could be driven by a different, though related, approach.

ISO standards, (ISO 281, 1990) considers, after (Lundberg, 1947) the maximum *alternating* shear stress as the critical factor on sub-surface bearing fatigue.

The shear stress parallel to the surface, τ_{yz} , actually reaches a maximum, τ_{yz-max} , at a point near the edge of the contact area (y/b almost 1, see sl. 13) and changes sign as the rolling element passes through the loaded contact zone.

The calculated depth of this critical point is slightly closer to the surface (0.50 b vs. 0.78 b) than with the maximum shear theory. Moreover, as seen in the next slide, the range is $\Delta\tau_{zy}=0{,}5$ i.e. higher than the max tangential stress at depth b=0,78 b, which ranges from zero to τ_{max}.

This is described in the next three slides.
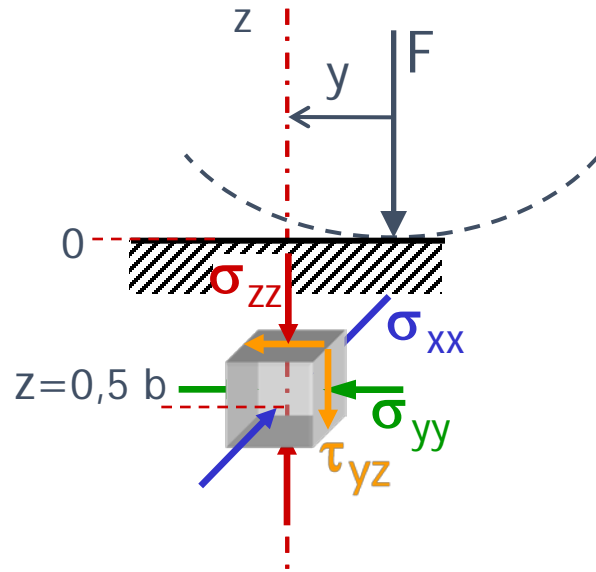
The figure on the right shows the deformed half-space and three sample infinitesimal elements (evidently enormously enlarged) at different distances from the vertical of the load F; for clarity only shears have been represented, the other stresses omitted.

The complete set of stresses (in their effective direction) is represented in the left-high figure.

In this introductory slide, we see a cylinder rolling on a plane surface. However we already know that it is not necessary this surface to be plane, it suffices that the relative curvature be the same (Ch.1 Sect.3 sl.2).
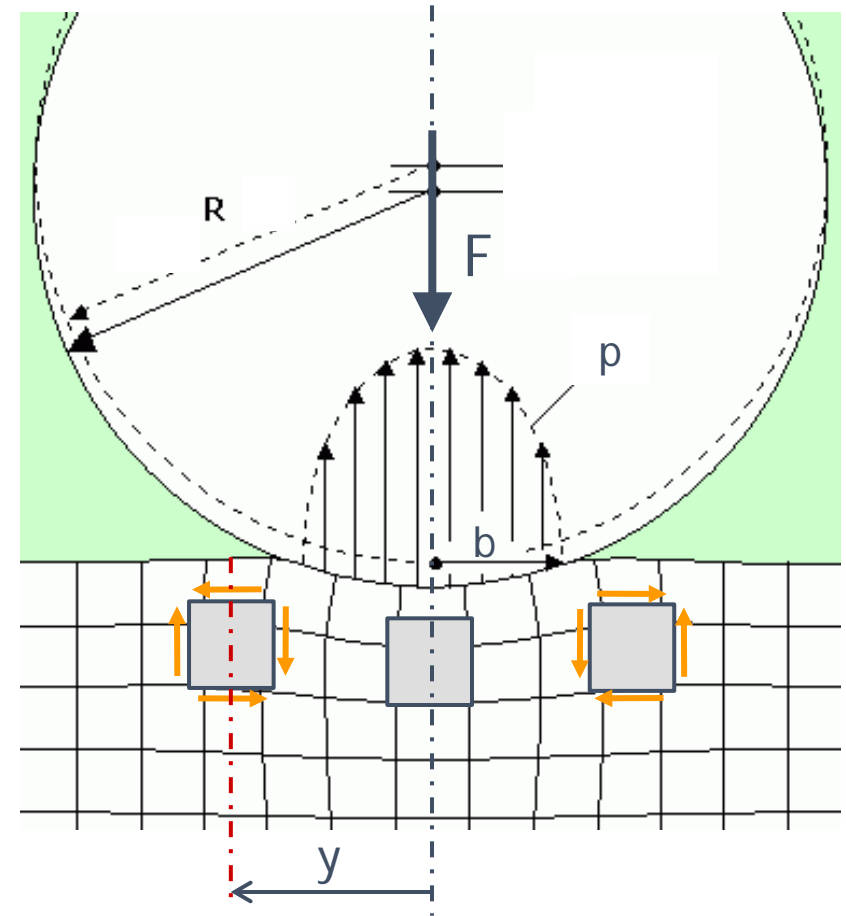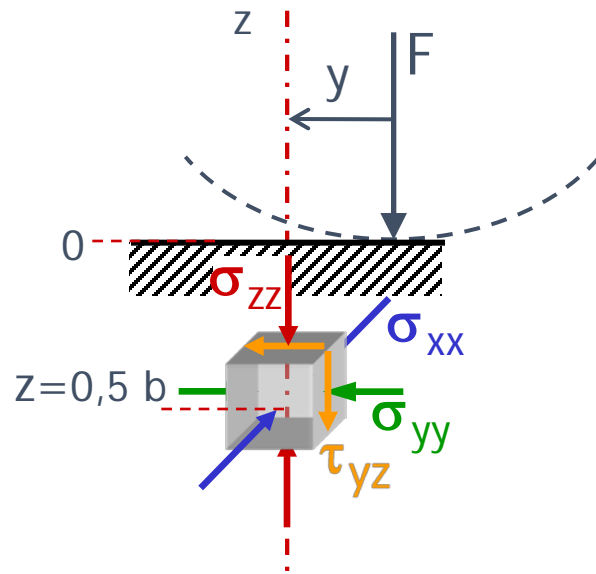
Rolling contact of elastic-plastic cylinders.
Solid line ——— : elastic stresses at depth z=0,5 b.
Broken line --- : with addition of $(\sigma_y)_r$ and $(\sigma_x)_r$
i.e. with residual stresses
(after shakedown)

σ/p_{max}

τ_{yz}/p_{max}

$\dfrac{\tau_{yz-max}}{p_{max}}$

y/b

σ_{xx}/p_{max}

σ_{yy}/p_{max}

$\dfrac{\sigma_{xx}+(\sigma_{xx})_r}{p_{max}}$

$\dfrac{\sigma_{yy}+(\sigma_{yy})_r}{p_{max}}$

σ_{zz}/p_{max}
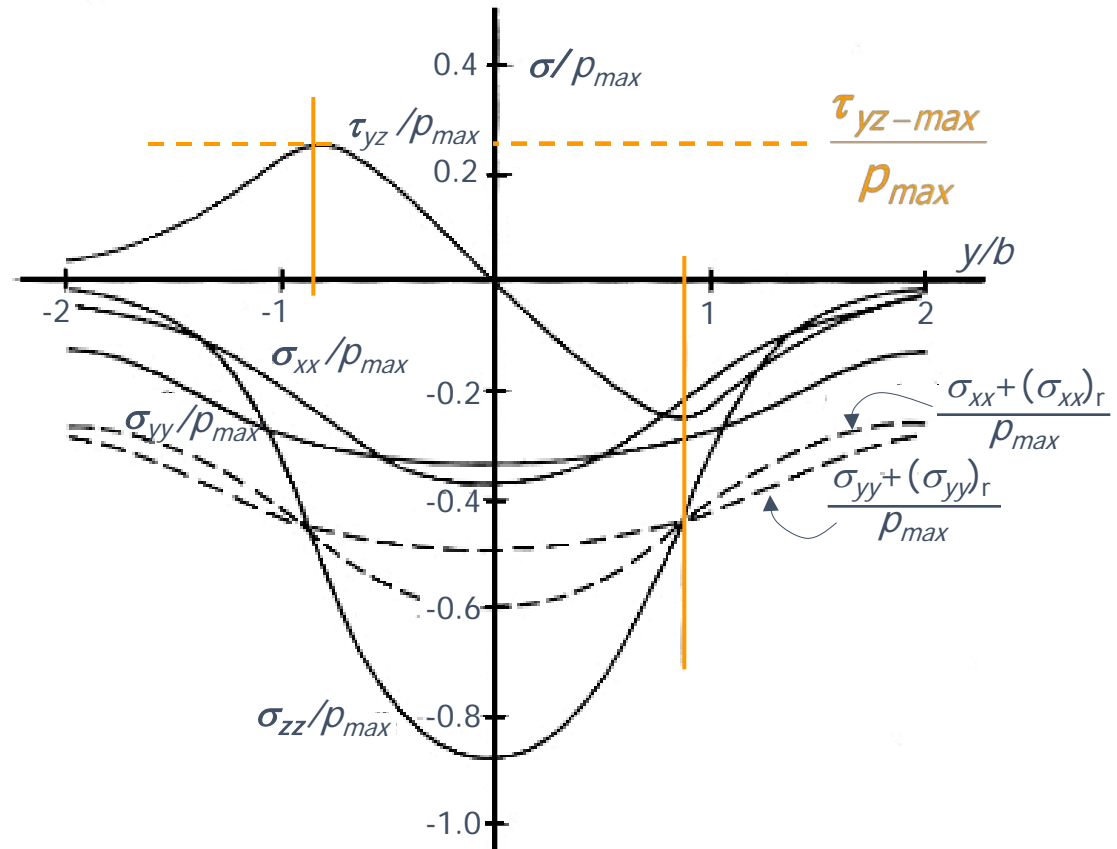
adapted from: K. L. Johnson, Contact Mechanics,
Cambridge University Press 2001

Rolling contact of cylinders.
Tangential stresses at: y=0, z=0,5b
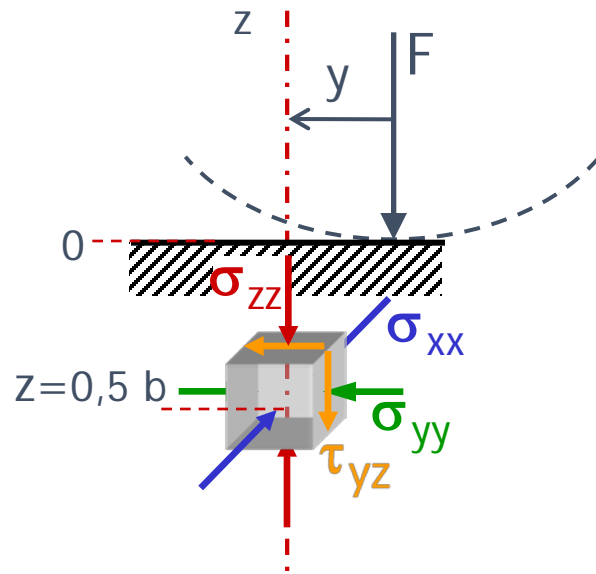
Here only shear stress is represented, for clarity; direction is according to conventional definition, sign is in the diagram on the right.

$(+y)$ τ_{yz}

$(-y)$ τ_{yz}
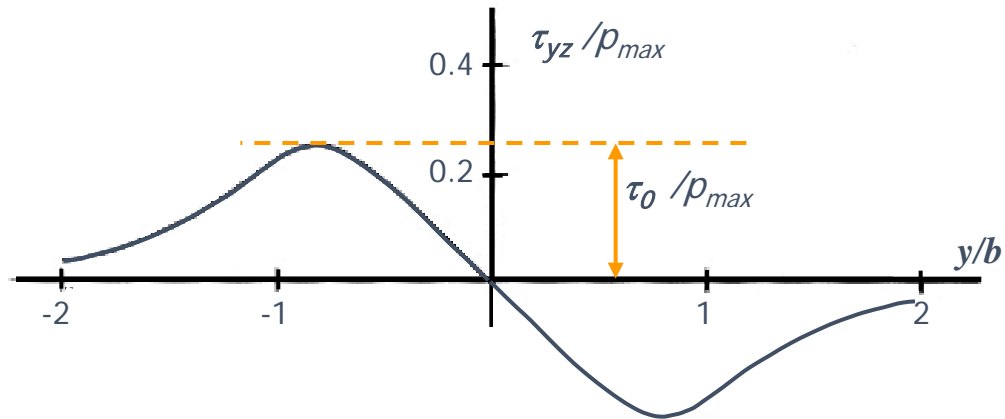
Later we shall employ the shorter symbol τ_0 for the max tangential stress amplitude at depth z_0 instead of $\tau_{yx\text{-}max}$.

τ_0 is the maximum alternating shear stress

When the rolling contact is at positive y then the tangential stresses on the element at y=0 , z=0,5 b (which are the highest) are as in the icon (+y), when the rolling contact is at negative y then tangential stresses are as in the icon (-y).

A common understanding is that fatigue is caused by the dynamic stressing of the material during cycling. However, there is not a general agreement on what parameters should explain fatigue.

Quoting Brändlein[*]:

Three hypotheses have been put forward: maximum shear stress, distortion energy and alternating shear stress.

The first hypothesis stipulates the maximum shear stress τ_H as the critical stress ... According to the distortion energy hypothesis, the material stressing is not governed by the stress conditions at a single point of the body but by those in a certain zone ..., and the distortion process below the surface is the characteristic feature. The location of the maximum distortion has been calculated ...; it coincides more or less with the location of the maximum shear stress. Therefore, when investigating fatigued bodies, it cannot be agreed upon which of the two hypotheses gives the best explanation for the fatigue process.

[*] Brändlein J., *Ball and Roller Bearings : Theory, Design, and Application*, 1999, John Wiley & Sons

According to the third hypothesis, the maximum alternating shear stresses, i.e. the orthogonal shear stresses, are responsible for the material fatigue ... This hypothesis is supported by the fact that most fatigue cracks in cycled components are found at a depth where the alternating shear stress τ_{yz} has reached its maximum ...

Since there is little difference in the effect of the individual hypotheses on practical rolling bearing calculations, the fatigue theory continues to be related to the alternating shear stress hypothesis. The fatigue theory on which the calculation methods for rolling bearings are based, now in common use and standardized by ISO, relates for historical reasons to the alternating shear stress hypothesis.

We may however remark that crack initiation and propagation are the effect of the whole sub-surface stress field, and not of a particular stress. The field stresses are all proportional to anyone of the stresses mentioned above; any of them can then be taken as a measure or an indicator of the stress field magnitude. In this sense, the maximum surface pressure could be considered as well.
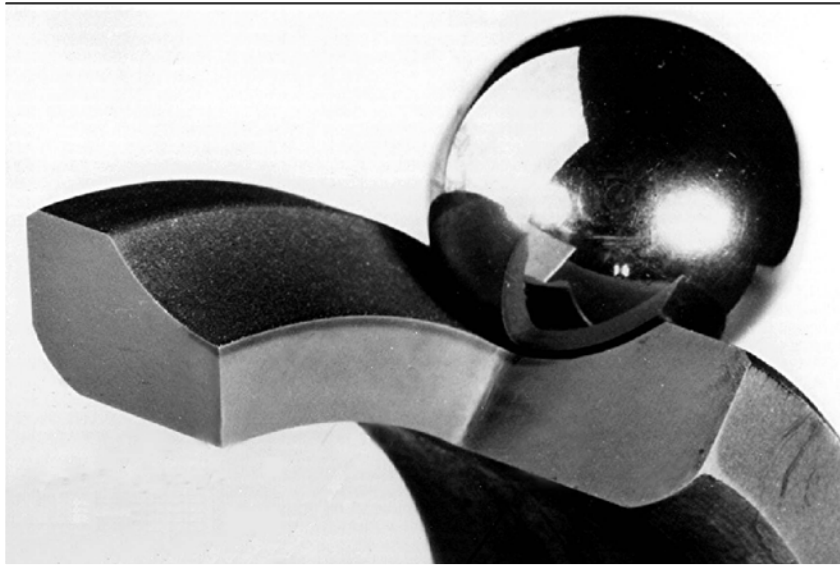
T. H. Harris, M. N. Kotzalas, Rolling Bearing Analysis, Taylor and Francis 2007, adapted
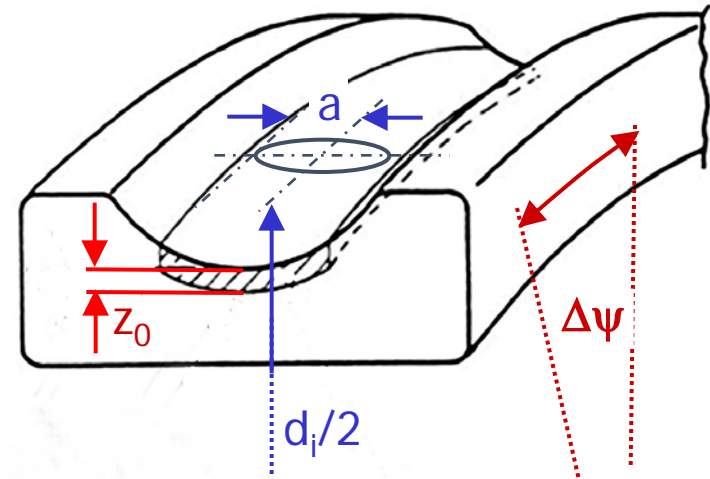
F. Sadeghi et al., A Review of rolling Contact Fatigue, ASME Jour. Tribol., 2009, adapted

The figures above show a section of the inner ring of a ball bearing; the volume ΔV_ψ at any angle ψ interested by stresses which may produce fatigue is proportional to depth z_0, semi-width a, and extends circumferentially by the length: $(d_i/2) \cdot \Delta \psi$.

On this basis, the elementary Weibull-Lundberg-Palmgren volume is defined as: $\Delta V_\psi = \xi \, z_0 \, a \, \dfrac{d_i}{2} \Delta \psi$

Lundberg and Palmgren supposed that a subsurface crack initiates due to the simultaneous occurrence, at a particular depth, of the maximum alternating (orthogonal) shear stress and a weak point in the material.

Such weak points were hypothesized to be stochastically distributed in the material.

> Subsurface initiated spalling, which is the classical mode of failure in rolling element bearings that operate under conditions of Elasto-Hydrodynamic-Lubrication, is significantly influenced by the material microstructure, which is inherently inhomogeneous due to the presence of defects and nonuniform distribution of material properties. As a result of these inhomogeneous material microstructures, spalling lives of a seemingly identical batch of bearings operating under identical load, speed, lubrication, and environmental conditions show a significant degree of scatter.

Sadeghi, F. et al., 2009, "A Review of Rolling Contact Fatigue," ASME Journal of Tribology, Vol. 131(4)

The Weibull statistical strength theory was applied to the stressed volume in a pure Hertzian contact to obtain the probability of survival of the volume from subsurface initiated fatigue.

Failure was assumed to be dominated by crack initiation.

For each elementary volume ΔV_ψ the survival probability (i.e., no crack initiated) is written by Weibull as:

$$S_\psi = 1 - f(\tau_0, N, z_0) \cdot \Delta V_\psi$$

where: τ_0 : max tangential stress amplitude at depth z_0

N : number of loading-unloading cycles

z_0 : depth

It is seen that the failure probability $f(\tau_0, N, z_0) \cdot \Delta V_\psi$ is proportional to the volume, i.e., the greater the volume the higher the probability that a material defect (such as a non-metallic inclusion) will find itself near the location of maximum stress.

For $i=1$ to k volumes ΔV_i the total probability (independent events $\Rightarrow$ product) is

$$S = S_1 \cdot S_2 \cdot \ldots S_i \cdot \ldots \cdot S_k = \prod_{i=1,k} \left[1 - f(\ldots) \Delta V_i \right]$$

whose logarithm is: $\ln S = \sum\limits_{i=1,k} \ln[1 - f(\ldots)\Delta V_i]$ (then we have a sum)

However, with: $f(\ldots)\Delta V_\psi \ll 1 \Rightarrow \ln[1 - f(\ldots)\Delta V_\psi] \cong -f(\ldots)\Delta V_\psi$

then: $\ln S = \sum\limits_{i=1,k} -f(\ldots)\Delta V_i$

in integral form: $\ln S = -\int\limits_V f(\ldots)dV$ (this the final reason for taking logarithms)

For the individual volume ΔV_ψ:

$$\ln S_\psi = -f(\ldots)\Delta V_\psi \quad \text{or} \quad \ln\frac{1}{S_\psi} = f(\ldots)\Delta V_\psi$$

Following Weibull, Lundberg and Palmgren introduced the empirical function:

$$f(\tau_0, N, z_0) = m \frac{\tau_0^c \, N^e}{z_0^h}$$

where m, c, e, h are material parameters to be later determined though comparisons between the predicted to the observed bearing fatigue life. The exponent "e" is the Weibull slope for the experimental life data plotted on a Weibull probability paper.

It may be worth mentioning that for the simplest case $f(...) \Delta V_\psi = \varphi N$ then:

$\ln S_\psi = -\varphi N$ gives $dS_\psi / S_\psi = -\varphi \, dN$, i.e.,   the variation in survival

probability is proportional to the survived population at that stage; it can also

be obtained from $S_\psi = e^{-\varphi N}$ whose variation is: $dS_\psi = -\varphi \, e^{-\varphi N} \, dN = -\varphi \, S_\psi \, dN$

It is exponential survival (or failure) distribution called "constant failure rate".

Applying the basic theory to the bearings, and considering only the raceways of a radial ball bearing, the volume is:

$$dV_\psi = \xi\, z_0\, a\, \frac{d_{i,o}}{2}\, d\psi \qquad \text{with} \begin{cases} d_{i,o} : \text{inner or outer raceway diameter} \\ \xi \quad : \text{geometrical shape factor} \end{cases}$$

Inner and outer raceway are to be treated separately.

For the **outer raceway**, consider here only the case where it is stationary, while the inner ring rotates with the shaft:
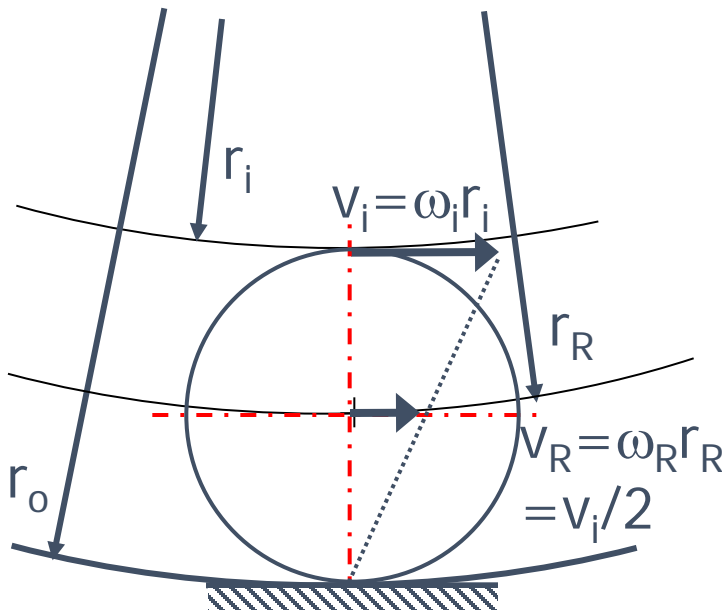
$$\omega_R = \frac{\omega_i\, r_i}{2\, r_R}$$

with Z rolling elements, over time t :

$$N = \frac{\omega_R\, t}{2\pi}\; Z = \frac{\omega_i\, t}{2\pi}\, Z\, \frac{r_i}{2\, r_R} = \tilde{L}\left(Z\, \frac{r_i}{2\, r_R}\right)$$

N : number of contacts on raceway

$\tilde{L}$: number of inner ring revolutions

Finally, relating shaft radial force R with contact loads:

$R = F_0 \, Z \, J_S$: J_S is the Stribeck integral (Ch. 2, Sect. 3, sl. 13)

$F_0 = \dfrac{R}{Z \, J_S}$: load on ball at $\psi = 0$

$F_\psi = \dfrac{R}{Z \, J_S} \left(\dfrac{\cos \psi - \cos \psi_{max}}{1 - \cos \psi_{max}} \right)$: load on ball at angle ψ

According to Hertz theory:

$\tau_0 = T \, p_{max}$; $z_0 = \varsigma \, a$; $p_{max} = P F_\psi^{1/3}$; $a = A F_\psi^{1/3}$

$\left. \begin{array}{l} T \\ \varsigma \\ P \\ A \end{array} \right\}$ constants

substitute:

$$\left. \begin{array}{l} \tau_0 = T \, p_{max} = T \cdot P F_\psi^{1/3} \\[2mm] z_0 = \varsigma \, a = \varsigma \cdot A F_\psi^{1/3} \\[2mm] N = \tilde{L} \, Z \, \dfrac{r_i}{2r_R} \equiv \tilde{L} \, u_o \end{array} \right\}$$

into: $\ln S_o = - \displaystyle\int_{-\psi_{max}}^{\psi_{max}} m \, \dfrac{\tau_0^c \, N^e}{z_0^h} \, dV_\psi$

The argument of the integral is then:

$$m \frac{\left(TPF_\psi^{1/3}\right)^c \left(\widetilde{L}\, u_o\right)^e}{(z_0)^h} \xi\, z_0\, a\, \frac{d_o}{2}\, d\psi = m \frac{\left(TPF_\psi^{1/3}\right)^c \left(\widetilde{L}\, u_o\right)^e}{(z_0)^{h-1}} \xi\, a\, \frac{d_o}{2}\, d\psi =$$

$$= m \frac{T^c P^c u_o^e d_o}{2\, z_0^{h-1} a^{h-2}}\; F_\psi^{1/3}\; \widetilde{L}^e\, d\psi = m \frac{T^c P^c u_o^e d_o}{2\, z_0^{h-1} A^{h-2}}\; F_\psi^{\frac{c-h+2}{3}}\; \widetilde{L}^e\, d\psi =$$

$$= m \frac{T^c P^c u_o^e d_o}{2\, z_0^{h-1} A^{h-2}} \left(\frac{1}{Z\, J_S}\right)^{\frac{c-h+2}{3}} \left(\frac{\cos\psi - \cos\psi_{max}}{1-\cos\psi_{max}}\right)^{\frac{c-h+2}{3}} R^{\frac{c-h+2}{3}}\, \widetilde{L}^e\, d\psi$$

Then the survival probability for the outer raceway is:

$$\ln S_o = - \int_{-\psi_{max}}^{\psi_{max}} m \frac{\tau_0^c N^e}{z_0^h} dV = -R^{\frac{c-h+2}{3}} \tilde{L}^e \int_{-\psi_{max}}^{\psi_{max}} [\ldots] d\psi = -J_o \ R^{\frac{c-h+2}{3}} \tilde{L}^e$$

which is shortly written: $\ln S_o = -J_o \ R^r \tilde{L}^e$ with: $\left(r = \frac{2c-h+2}{3} \right)$

The inner raceway produces a formula with the same structure and exponents, however with a different coefficient: $\ln S_i = -J_i \ R^r \tilde{L}^e$

With L for "millions of revolutions", in summary:

$$\ln S_i = -\tilde{J}_i \ R^r L^e$$

$$\ln S_o = -\tilde{J}_o \ R^r L^e$$

Reminder:
S_i , S_o : inner and outer ring survival probabilities
R : radial load
L : inner ring millions of revolutions

Starting from the final formulas of sl. 9:

$$\ln S_o = -\tilde{J}_o \, R^r L^e \qquad \ln S_i = -\tilde{J}_i \, R^r L^e$$

$$S_o = e^{-\tilde{J}_o \, R^r L^e} \qquad S_i = e^{-\tilde{J}_i \, R^r L^e}$$

the joint survival probability for inner and outer ring is:

$$S = S_o \, S_i = e^{-\left(\tilde{J}_o + \tilde{J}_i\right) R^r L^e} \equiv e^{-J \, R^r L^e}$$

This equation is used in two ways:

a) given reliability (e.g. S=0,9)

$$0,9 = e^{-J \, R^r L_{10}^e} \implies \ln 0,9 = -J \, R^r L_{10}^e$$

$$R^r L_{10}^e = -\frac{\ln 0,9}{J} \implies R^p \, L_{10} = C^p$$

Load-life equation

b) given radial load

$$S = e^{-\chi \cdot L_{(1-S)}^e}$$

i.e. $\dfrac{\ln S}{\ln 0,9} = \left(\dfrac{L_{(1-S)}}{L_{10}}\right)^e$

Reliability equation

Note: $L_{(1-S)}$ is the number of inner ring million revolutions for a survival probability S , i.e., a failure probability 1-S .

Inner raceway, complement 1

Frequency of contacts on the inner raceway: giving to the whole bearing a counter-rotation $-\omega_i$ so to keep the inner ring stationary, the cage will rotate backwards with a rotational speed $-(\omega_i - \omega_R)$ and the force vector R with a rotational speed $-\omega_i$.
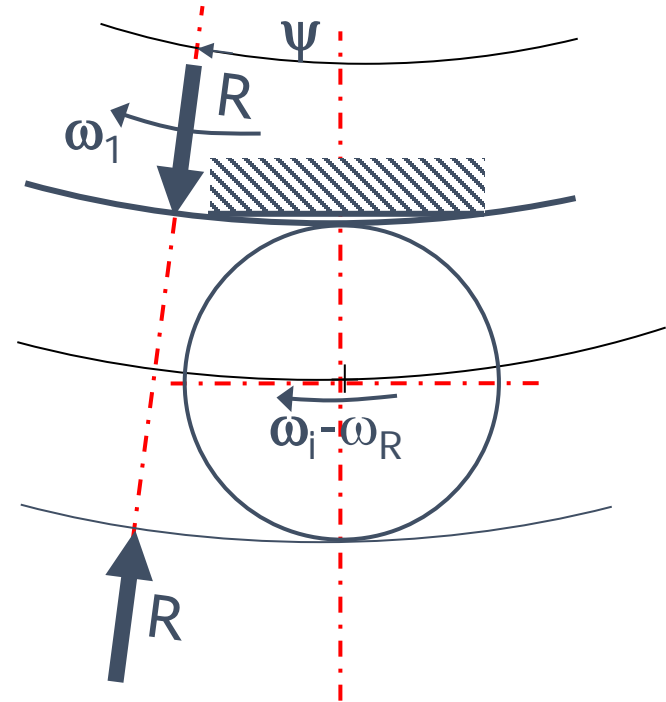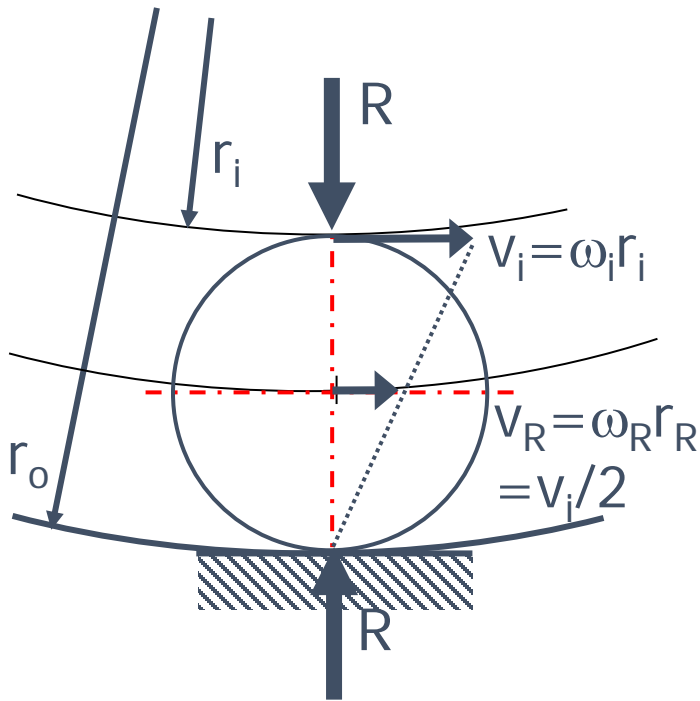
Then the total number of contacts N on any point of the inner raceway is:

$$N = \frac{\omega_i - \omega_R}{2\pi} Z\, t = \frac{\omega_i}{2\pi} Z\, \frac{2r_R - r_i}{2\, r_R} t = \tilde{L}\left(Z\, \frac{2r_R - r_i}{2\, r_R} \right) = \tilde{L} u_i$$

Inner raceway, complement 2a

Inner raceway equivalent contact force: the radial force R rotates relative to the inner rings with a speed which is different from that of the centers of balls, wich coincides with the speed of the ball-raceway contact points.

We cannot expect - due to manufacturing tolerances - that the ratio of the two rotation velocities of inner and outer ring be exactly the ratio of two integers, then the contact at a given point will not take place for a discrete set of angles ψ between R and contact point.

We can assume that all values of contact forces will be present, through the whole bearing life, on the raceway arc $d\psi$ for an equal number of cycles

contact force distribution

contact number distribution
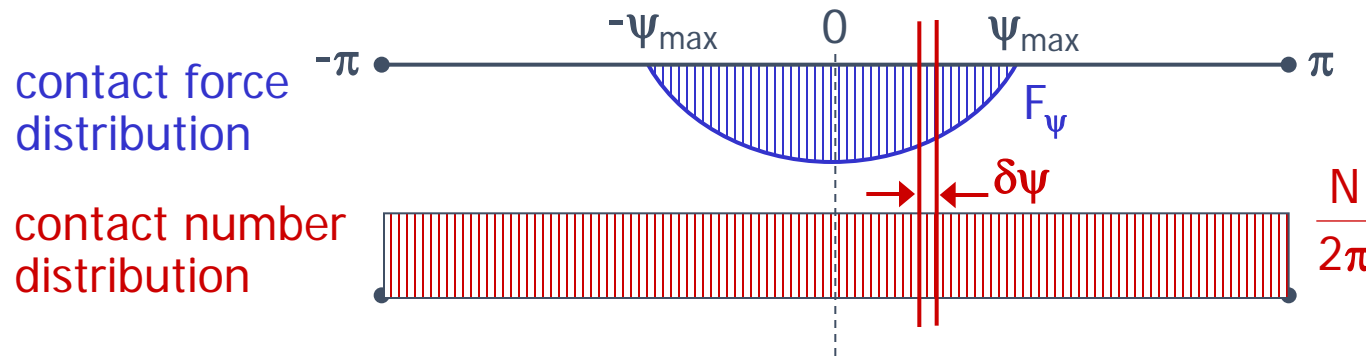
$$dN_\psi = \frac{N}{2\pi} d\psi$$

Inner raceway, complement 2b

For any chosen survival probability S_i , radial load R and total number of load cycles: $F^r N^e = \text{constant}$, or : $F^p N = \widetilde{C}^p$

According to Miner's rule the fractional damage is proportional to: $\dfrac{dN_\psi}{N_\psi}$

where N_ψ is the maximum number of cycles at damage (with survival probability S_i) for the applied load F_ψ ; then damage occurs when:

$$\int_{-\pi}^{\pi} \frac{dN_\psi}{N_\psi} = 1 \quad \Rightarrow \quad \int_{-\pi}^{\pi} \frac{1}{N_\psi} \frac{N}{2\pi} d\psi = \frac{N}{2\pi} \int_{-\pi}^{\pi} \frac{1}{N_\psi} d\psi = 1$$

with : $F_\psi^p N_\psi = \widetilde{C}^p$

$$\frac{N}{2\pi} \int_{-\pi}^{\pi} \frac{F_\psi^p}{\widetilde{C}^p} d\psi = 1 \Rightarrow \frac{N}{2\pi} \int_{-\pi}^{\pi} F_\psi^p d\psi = \widetilde{C}^p \quad \text{then :} \quad \frac{1}{2\pi} \int_{-\pi}^{\pi} F_\psi^p d\psi \equiv \frac{1}{2\pi} \int_{-\psi_{max}}^{\psi_{max}} F_\psi^p d\psi = F_{eq}^p$$

F_{eq} is the constant "equivalent" load which produces the same damage on all arcs $d\psi$ of the inner raceway; it will be: $F_{eq} = J_M R$, with J_M "Miner integral".

The first important functional relation resulting from the Lundberg and Palmgren development***** of the Weibull approach to fatigue is the load-life equation, i.e., the equation which relates the bearing fatigue life to the applied load for a standard :

$$R^p L_{10} = C^p$$

which is normally written:

$$L_{10} = \left(\frac{C}{P}\right)^p$$

L_{10} : basic rating life - 10^6 inner ring revs - at 90% (S=0,9) reliability
i.e. only 10% of bearings will fail at $L < L_{10}$ million cycles

C : basic dynamic capacity, i.e., load at which the bearing
has a nominal service life of one million revs

P : equivalent dynamic load $P = X R + Y A$

p : load–life exponent, determined experimentally at 3 for
ball bearings and 10/3 for cylindrical roller bearings

*G. Lundberg and A. Palmgren, "Dynamic Capacity of Rolling Bearings" *Acta Polytechnica Mech. Eng. Series,* 1,3,(1947)

The basic dynamic capacity C for a given bearing is given in the catalogue; it is a function of bearing internal geometry, type of loading applied to the bearing (either simple radial or simple thrust loading or a combination of the two) and ring and rolling element materials.

For ball bearings, internal geometry includes only ball diameter, pitch diameter and raceway groove radii. For roller bearings, roller diameter replaces ball diameter and the internal geometry includes the effective length of contact between rollers and raceways.

Cylindrical rollers are crowned to eliminate edge loading, and are generally characterized by nominal contact length L_c and a crown radius R. The self-aligning "spherical" rollers are characterized by the ratio of the roller contour radius to the raceway contour radius, i.e. osculation, transverse to rolling motion. Depending on the roller–raceway load for a given osculation, the roller may experience contact over its entire length or over only a portion of the length.

To accommodate variation in the type of contact, the load–life exponent p in the case of roller bearings was established by Lundberg and Palmgren to the value 10/3 .

In the 1960s, with the advent of improved cleanliness, commercial ball bearing steels, e.g. vacuum degassed AISI 52100 steels, and ultra-clean Vacuum Induction-Melted / Vacuum-Arc-Remelted (VIM / VAR) aircraft bearing steels, it was recognized that the load-life equations for ball and roller bearings predicted substantially shorter fatigue lives than were actually occurring in applications.

Accordingly, the following equation was proposed (ISO 281/1-1977) to predict bearing fatigue endurance better:

a: adjusted

$$L_{na} = a_1 \cdot a_2 \cdot a_3 \cdot L_{10} = a_1 \cdot a_2 \cdot a_3 \cdot \left(\frac{C}{P}\right)^p \quad \text{also written} = a_1 \cdot a_{23}\left(\frac{C}{P}\right)^p$$

adjustment factor for operating conditions (lubrication)

adjustment factor for the material

life adjustment factor for the selected reliability level

n=% failure probability, i.e., 100(1-S)

The equation for SKF rating life is in accordance with ISO 281:1990 / Amendment 2:2000 :

$$L_{na} = a_1 \cdot a_{SKF} \cdot \left(\frac{C}{P}\right)^P$$

The SKF life modification factor a_{SKF} applies the concept of fatigue load limit P_u analogous to that used when calculating other machine components (in bearings, asymptotic infinite life evaluated at 10^{11} cycles). It is underlined that while a_{23} was independent of load P, the newer a_{SKF} factor depends on the ratio P_u/P through the load parameter:

$$\frac{P - P_u}{C}$$

The values of the fatigue load limit P_u are provided in the SKF product tables. Furthermore, the SKF life modification factor a_{SKF} makes use of the lubricant conditions (viscosity ratio κ) and a factor η_c for the contamination level to reflect the application's operating conditions.

Finally, for high operating temperatures further corrections are needed that require direct contacts with the manufacturer's technical services.

In the area of interest to mechanical applications, the ratio $a_1 = L_{na}/L_{10}$ - life adjustment factor - for different "n" failure % probabilities is (from SKF catalog; see also formulas in Sect. 4):

S: survival probability	$a_1 = L_n/L_{10}$	$n = 100(1-S)$ failure % prob.
0,90	1	10
0,95	0.62	5
0,96	0.53	4
0,97	0.44	3
0,98	0.33	2
0,99	0.21	1

Calculated with:

$$\frac{L_n}{L_{10}} = \left(\frac{\ln S}{\ln 0.9} \right)^{2/3}$$

The reliability equation: $S = e^{-\chi \cdot L_{1-S}^{e}} \equiv e^{-\chi \cdot L_n^{e}} \Rightarrow \ln S = -\chi \cdot L_n^{e}$

when S=0,9 gives: $\qquad 0,9 = e^{-\chi \cdot L_{10}^{e}} \Rightarrow \ln 0,9 = -\chi \cdot L_{10}^{e}$

hence: $\qquad \dfrac{\ln S}{\ln 0,9} = \left(\dfrac{L_n}{L_{10}} \right)^{e}$ (compare at Sect.2, sl.10)

takes today the modified and improved form:

$$S = e^{-0,105 \cdot \left(\frac{L_n - L_0}{L_{10} - L_0} \right)^{e}} \qquad (-0.105 = \ln 0,9)$$

S : survival probability for the total duration L

L : total number of bearing revolutions (in 10^6 rev)

L_0: minimum bearing life (in 10^6 rev)

L_{10}: basic life, i.e., the life of reached by at least 90% of the bearings, i.e. n=10% failure probability, (in 10^6 rev)

According to Lundberg and Palmgren $e = 10/9$ for ball bearings and $e = 9/8$ for roller bearings. For modern, ultraclean, vacuum-remelted steels, values of e in the range 0.7–3. 5 have been found.

The value of L_0 was taken to be 0 in the past, today $L_0 \cong 0.05 L_{10}$.
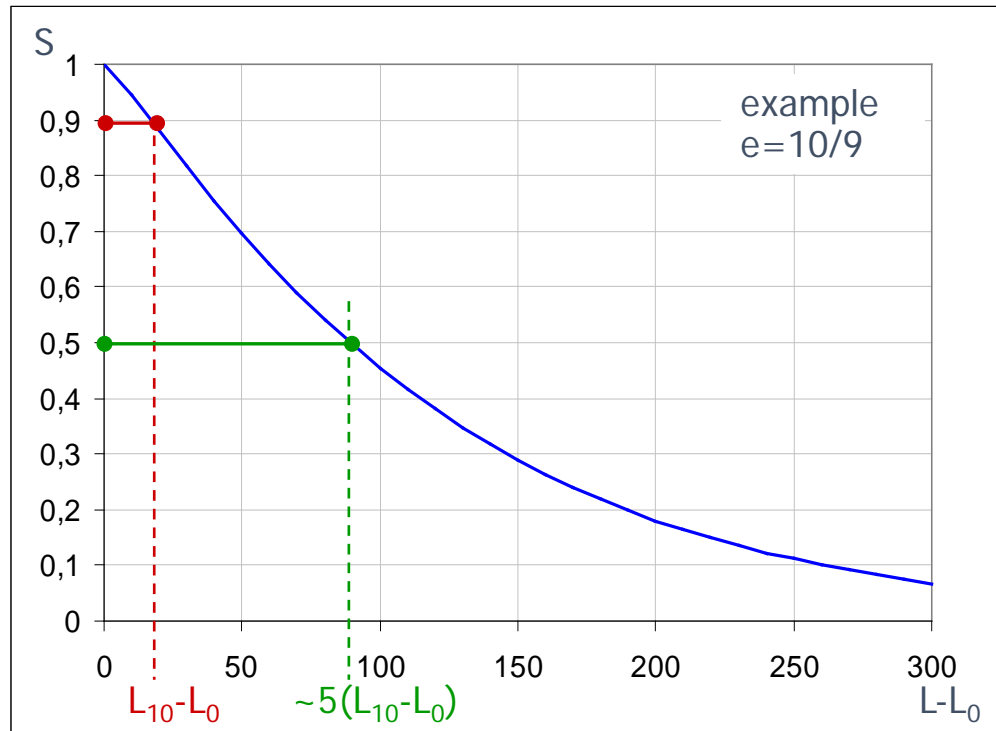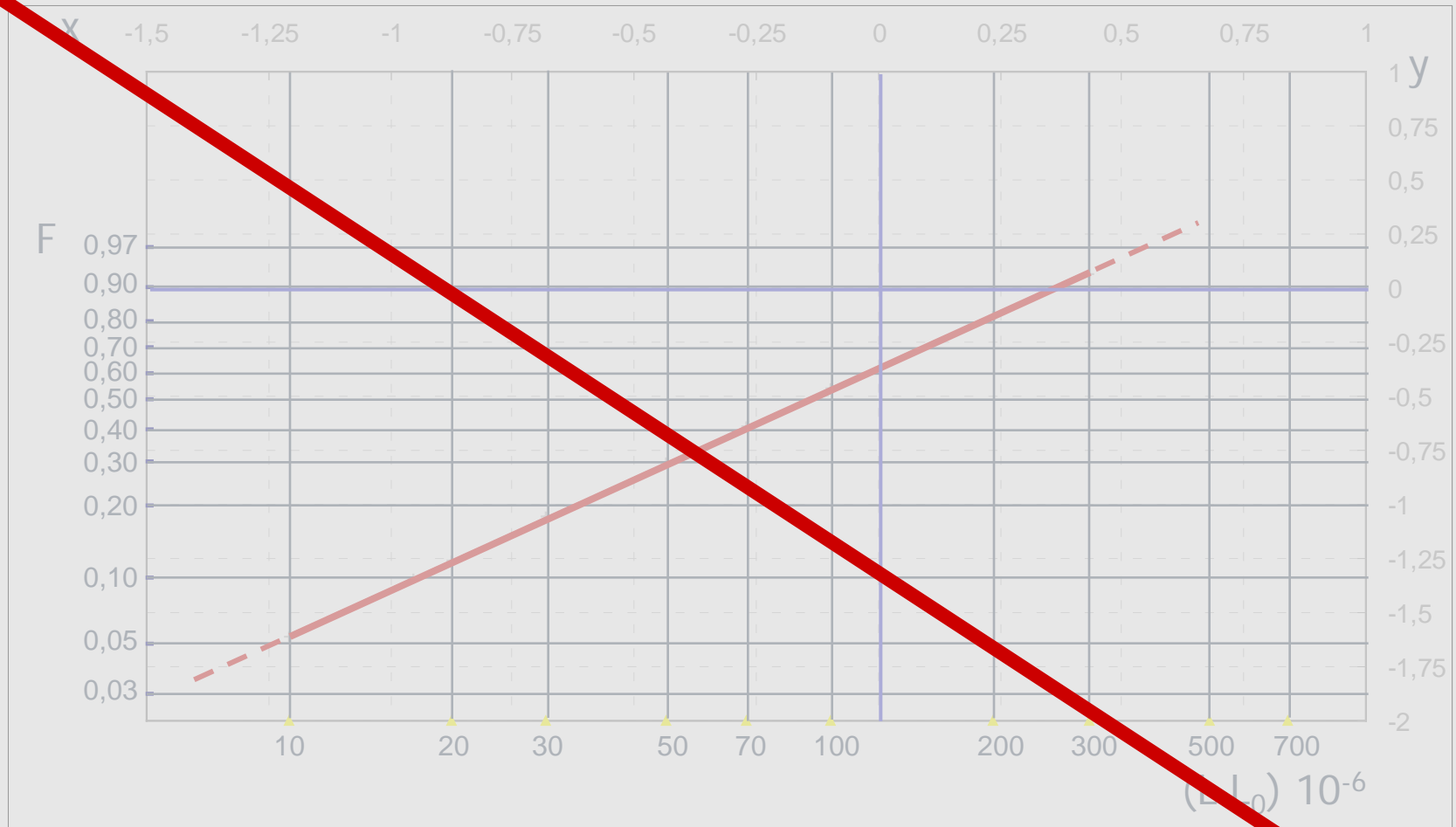

The survival probability:

$$S = e^{-0,105 \cdot \left(\frac{L_n - L_0}{L_{10} - L_0} \right)^e}$$

is transformed into:

$$\frac{L_n}{L_{10}} = 0,05 + 0,95 \left(\frac{\ln S}{\ln 0.9} \right)^{\frac{1}{e}}$$
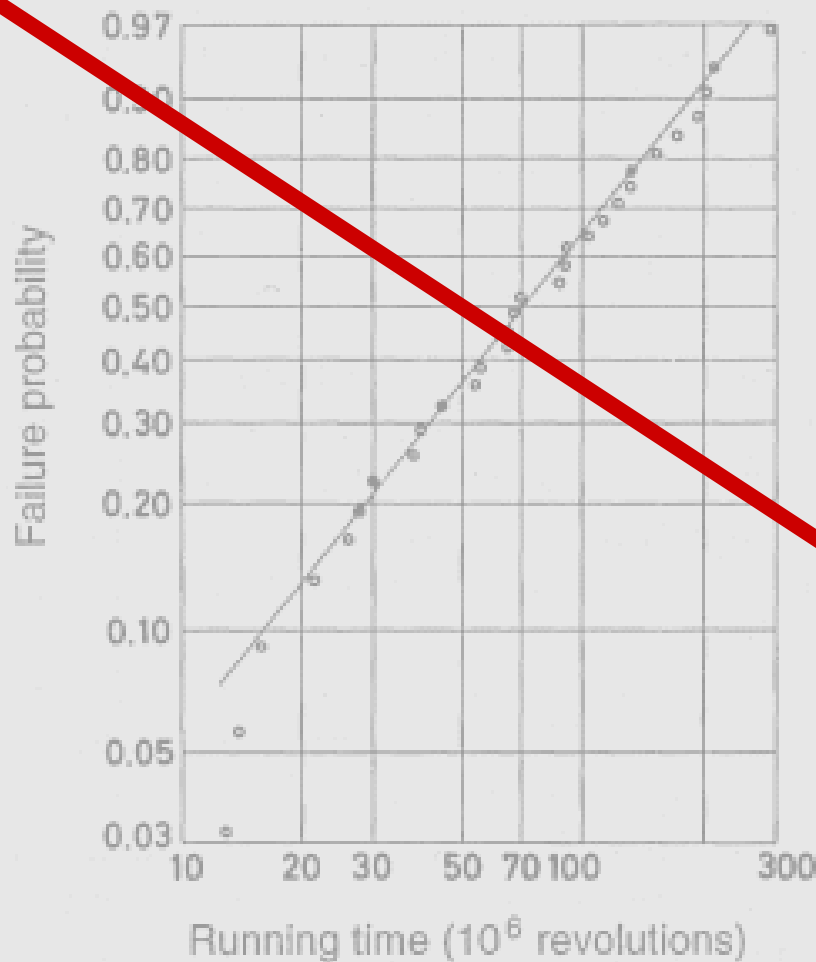
Slide incomplete, section under development

$$y = \text{Log}\left(\text{Log}\left(\frac{1}{1-F}\right)\right)$$

Experimental points in this figure (from Brändlein*) compare with the ISO formula predictions.

We see that 10% of the bearings examined had failed after 17 million revolutions and 50% after 70 million.

Brändlein remarks that: *fatigue tests carried out with very large bearing groups have shown that the straight line on the Weibull plot in the range from 0.07 to 0.6 failure probability is in very good agreement with the test results. Outside this range, below as well as above, the fatigue lives are longer.*

*Source: J. Brändlein, *Ball and Roller Bearings: Theory, Design and Application*, John Wiley & Sons 1999

Slide incomplete, section under development

Most bearings are operated under combinations of variable loading and speed. Palmgren recognized that the variation in both load and speed must be accounted for in order to predict bearing life. He reasoned:
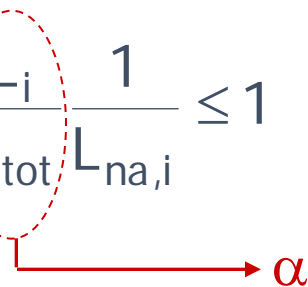
"*In order to obtain a value for a calculation the assumption might be conceivable that (for) a bearing which has a life of n million revolutions under constant load at a certain rpm (speed), a portion m/n of its durability will have been consumed. If the bearing is exposed to a certain load for a run of m_1 million revolutions where it has a life of n_1 million revolutions, and to a different load for a run of m_2 million revolutions where it will reach a life of n_2 million revolutions, and so on, we will obtain:*

$$\frac{m_1}{n_1} + \frac{m_2}{n_2} + \frac{m_3}{n_3} + \ldots = 1$$

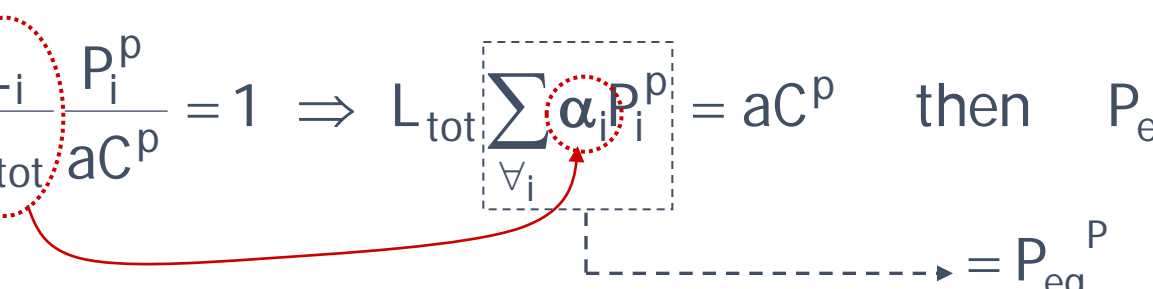This equation was independently proposed for conventional fatigue analysis by Miner at Douglas Aircraft in 1945, 21 years after Palmgren. The equation has been subsequently referred to as the "linear damage rule" or the "Palmgren-Miner rule".

In bearings it takes the form:

$$\sum_{\forall i} \frac{L_i}{L_{na,i}} \leq 1 \Rightarrow L_{tot} \sum_{\forall i} \underbrace{\frac{L_i}{L_{tot}}}_{\alpha_i} \frac{1}{L_{na,i}} \leq 1$$

If: $L_{na,i} = a_1 a_{23} \left(\frac{C}{P_i}\right)^p = a\left(\frac{C}{P_i}\right)^p$ with constant coefficients a_1, a_{23}

$$L_{tot} \sum_{\forall i} \frac{L_i}{L_{tot}} \frac{P_i^p}{aC^p} = 1 \Rightarrow L_{tot} \sum_{\forall i} \alpha_i P_i^p = aC^p \quad \text{then} \quad P_{eq} = \sqrt[p]{\sum_{\forall i} \alpha_i P_i^p}$$

$$= P_{eq}^p$$

...where P_{eq} has the meaning of "equivalent load", i.e., a radial constant load that, when applied for the total number of cycles L_{tot}, would produce the same damage of P_i each applied for its number of cycles L_i (see Sect. 3 sl. 1) .

If: $L_{na,i} = a_1 a_{SKF} \left(\dfrac{C}{P_i} \right)^p$ with a_{SKF} dependent on load P_i , then a

concise formula for P_{eq} can no longer be obtained, and only the

following can be used:

$$L_{tot} \sum_{\forall i} \alpha_i \frac{1}{L_{na,i}} \leq 1 \quad \Rightarrow \quad L_{tot} \leq \frac{1}{\displaystyle\sum_{\forall i} \frac{\alpha_i}{L_{na,i}}}$$

α_i is the utilisation fraction

(compare with Vol. 1 – Fatigue - Chapter 2, Sect. 14)

Modern rolling-element bearing steel and metallurgy do not begin until about 1856 with the disclosure of the Bessemer process. In this process air is blown through molten pig iron to produce a relatively high grade of steel.

This was followed ten years later by the introduction of open-hearth melting (also called Siemens-Martin Process) which further improved quality and made steel far more accessible to industry.

The use of carbon and chromium steels for bearings gradually increased during the last quarter of the 19th Century as the need for bearings capable of reliably supporting heavy loads increased.

The need was to have a steel hardened throughout and uniformly hard and tough.

A classical "high speed" tool steel, "through hardening", introduced around 1900, is ASTM-A295 (ASTM=American Society for Testing Materials), also named AISI 52100 (AISI=American Iron and Steel Institute) or DIN100Cr6, SUJ2, EN31 etc.

Its composition in % is:

C	Mn	Si	Cr
0.98~1,10	0.25~0,45	0.15~0,35	1,30~1,60

From 1953-54, steel AISI M50 was developed and introduced. It is an intermediate high speed tool steel, through hardening. Today commonly produced by VIM-VAR methods, ir is also known as LESCALLOY® M50 VIM-VAR.

	C	Mn	Si	Cr	Ni	V	Mo	W
M50	~0.80	~0.25	<0.25	~4.00	<0.15	~1.00	~4.25	<0,25

Widely used for critical aircraft engine bearings operating at elevated temperatures, the AISI M50 family has good hot hardness and excellent rolling contact fatigue strength.

It is ideal for highly stressed parts such as bearings and gears up to 700÷800°F (371÷427 °C).

Carburizing-grade steels

"Through-hardened materials, heat treated to Rockwell C 60 hardness, as is typical with bearing components, have limited fracture toughness. Applications requiring higher toughness will have to be made from a carburizing-grade steel. Carburizing-grade steels have reduced carbon content so that heat treatment normally results in moderate hardness and high toughness."

"High surface hardness, which is required for rolling-element bearing performance, is achieved by diffusing carbon into the surface, a process called carburizing, prior to heat treatment. Locally the steel is then a high-carbon alloy and is heat treatable to full hardness. The resulting structure has a surface layer with mechanical properties that are equivalent to those of traditional through-hardened bearing steels and a core that remains at low hardness, with corresponding high ductility and high fracture toughness." *

*Zaretsky E.V., Rolling Bearing Steels - A Technical and Historical Perspective, NASA/TM—2012-217445, 2012
http://ntrs.nasa.gov/archive/nasa/casi.ntrs.nasa.gov/20120008557_2012008568.pdf

"*Surface-initiated defects (e.g., a spall) propagate cracks into the tough core before they reach critical size. The tough core prevents rapid and catastrophic fracture ...*

... Fracture toughness of a material is inversely proportional to its carbon content and hardness ... Fracture toughness can be improved without affecting hardness by adding nickel ... Adding nickel also influences carbide size and distribution within the steel, which affects fatigue life ...

... Recognizing this, Bamberger (1983) modified the chemistry of AISI M-50 steel by decreasing the amount of carbon and increasing the amount of nickel. He called this modified AISI M-50 steel M50 NiL (the "Ni" referring to increased nickel and the "L" to low carbon). The steel is also designated as Aerospace Material Specification (AMS) 6268." *

* Zaretsky E.V., Rolling Bearing Steels - A Technical and Historical Perspective, NASA/TM—2012-217445, 2012
http://ntrs.nasa.gov/archive/nasa/casi.ntrs.nasa.gov/20120008557_2012008568.pdf

	C	Mn	Si	Cr	Ni	V	Mo	W
M50-NiL	~0.15	~0.25	<0.25	~4.0	~3.50	~1.25	~4.25	-

"M50 NiL, which is case carburized, has a core with a high fracture toughness K_{IC} (over 60 MPa -m$^{1/2}$; 50 ksi-in.$^{1/2}$) than through hardened AISI M-50 (29 MPa -m$^{1/2}$; 20 ksi-in.$^{1/2}$).

The M50 NiL core hardness is Rockwell C 43 to 45. M50 NiL has finer carbides (compounds of carbon and various alloying elements) dispersed more evenly within its microstructure than standard AISI M–50. Compressive residual stresses in excess of 210 MPa (30 ksi) are induced in the zone of maximum resolved shear stresses during carburization of M50 NiL.

These residual stresses combined with the fine carbide structure will increase its rolling-element fatigue life over that of conventional AISI M–50." *****

*Zaretsky E.V., Rolling Bearing Steels - A Technical and Historical Perspective, NASA/TM—2012-217445, 2012
http://ntrs.nasa.gov/archive/nasa/casi.ntrs.nasa.gov/20120008557_2012008568.pdf

According to Zaretsky, with improved bearing manufacturing and steel processing, together with lubrication technology, the potential improvements in bearing life can be as much as 80 times that attainable in the late 1950s or as much as 400 times that attainable in 1940.

Major advances in steel producing have occurred beginning in the 1950s by the introduction of vacuum-melting procedures. Vacuum processing reduces or eliminates the amount of nonmetallic inclusions, entrapped gases, and trace elements in structural alloys, resulting in substantially cleaner material.

The two primary methods of vacuum processing are vacuum induction melting (VIM) and consumable-electrode vacuum melting (CEVM) also called vacuum arc remelting (VAR).

In the early 1970s these two methods were combined, whereby the vacuum induction primary melt is vacuum arc remelted. This method, called VIM–VAR, produces much cleaner steel than either VIM or CEVM individually.

Rolling fatigue life as a function of steel processing, tested on a rolling specimen:

AM : air melting

VIM: vacuum induction melting

VAR: vacuum arc remelting

Vacuum processing of bearing steel increases bearing life by eliminating hard oxide inclusions that act as stress raisers to initiate incipient failure. This results in an un-foreseen secondary benefit. The fatigue life of the bearing steel becomes more sensitive to a reduction in stress. That is, as contact load or (Hertz) stress is decreased, bearing fatigue life is increased at a faster rate than with the air melted bearing steels. *
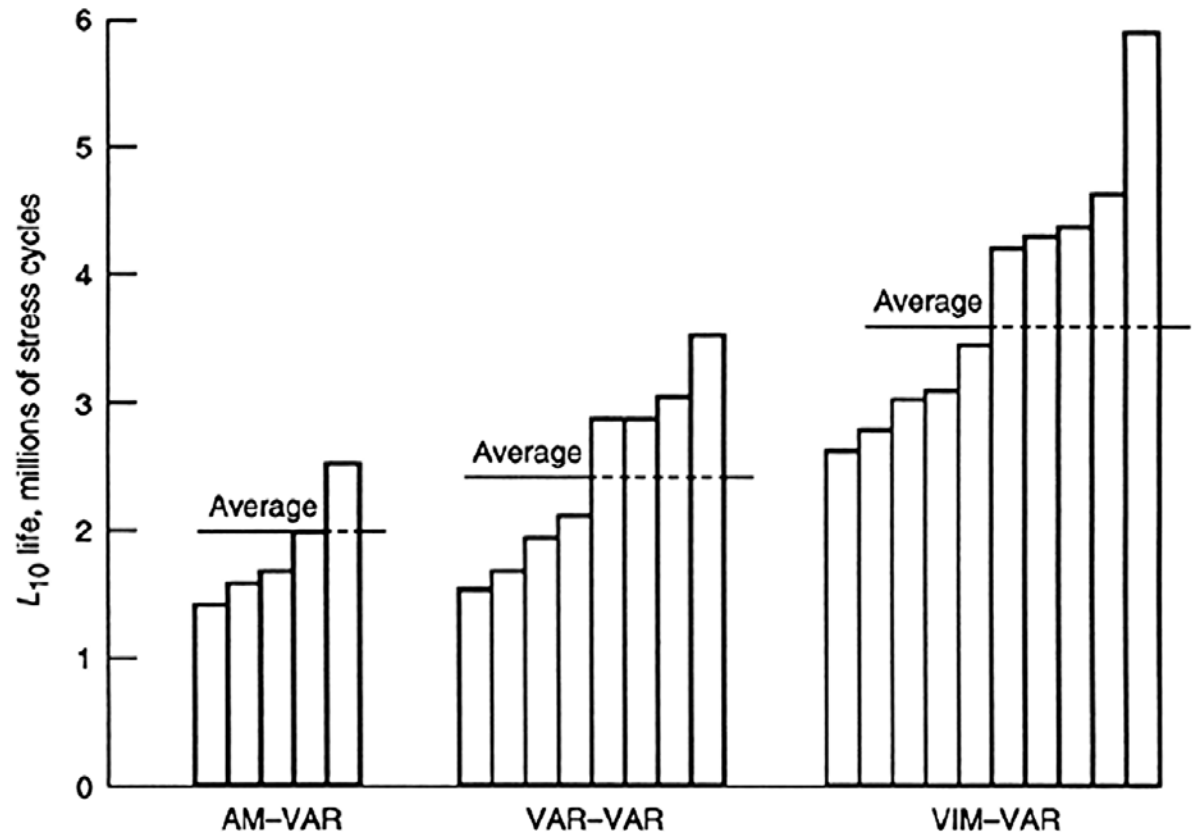
* Zaretsky E.V., Rolling Bearing Steels - A Technical and Historical Perspective, NASA/TM—2012-217445, 2012
http://ntrs.nasa.gov/archive/nasa/casi.ntrs.nasa.gov/20120008557_2012008568.pdf

Fatigue lives of the previous slides have been obtained using the five-ball tester shown in the figure on the right.

This fatigue tester consists essentially of an upper test ball pyramided on four lower balls that are positioned by a separator and are free to rotate in an angular-contact raceway.

System loading and drive are supplied through a vertical drive shaft, which grips the upper test ball. For every revolution of the drive shaft, the upper test ball receives three stress cycles from the lower balls.

The upper test ball and raceway are analogous in operation to the inner and outer races of a bearing, respectively.

The separator and lower balls function in a manner similar to the cage and the balls in a bearing.
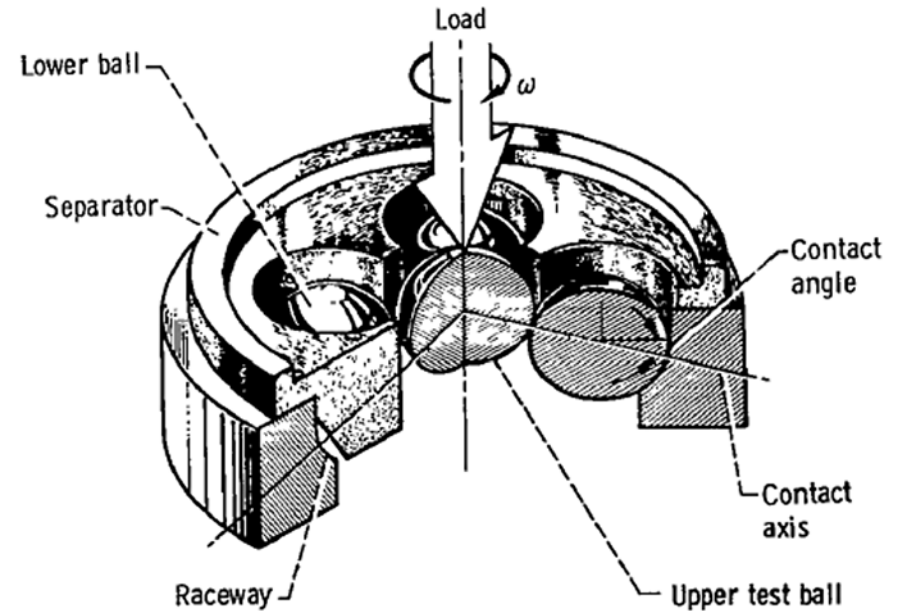
Parker R. J., Hodder R. S. , Effect of Double Vacuum Melting and Retained Austenite on Rolling-Element Fatigue Life of AMs *5749* Bearing Steel, NASA Technical Paper 1060, Oct. 1977
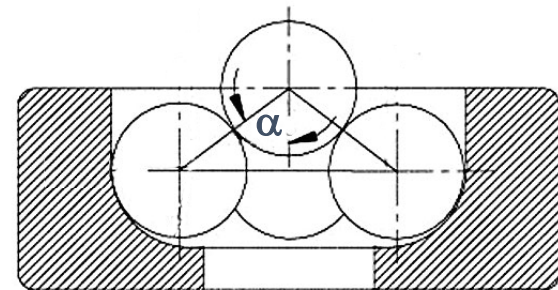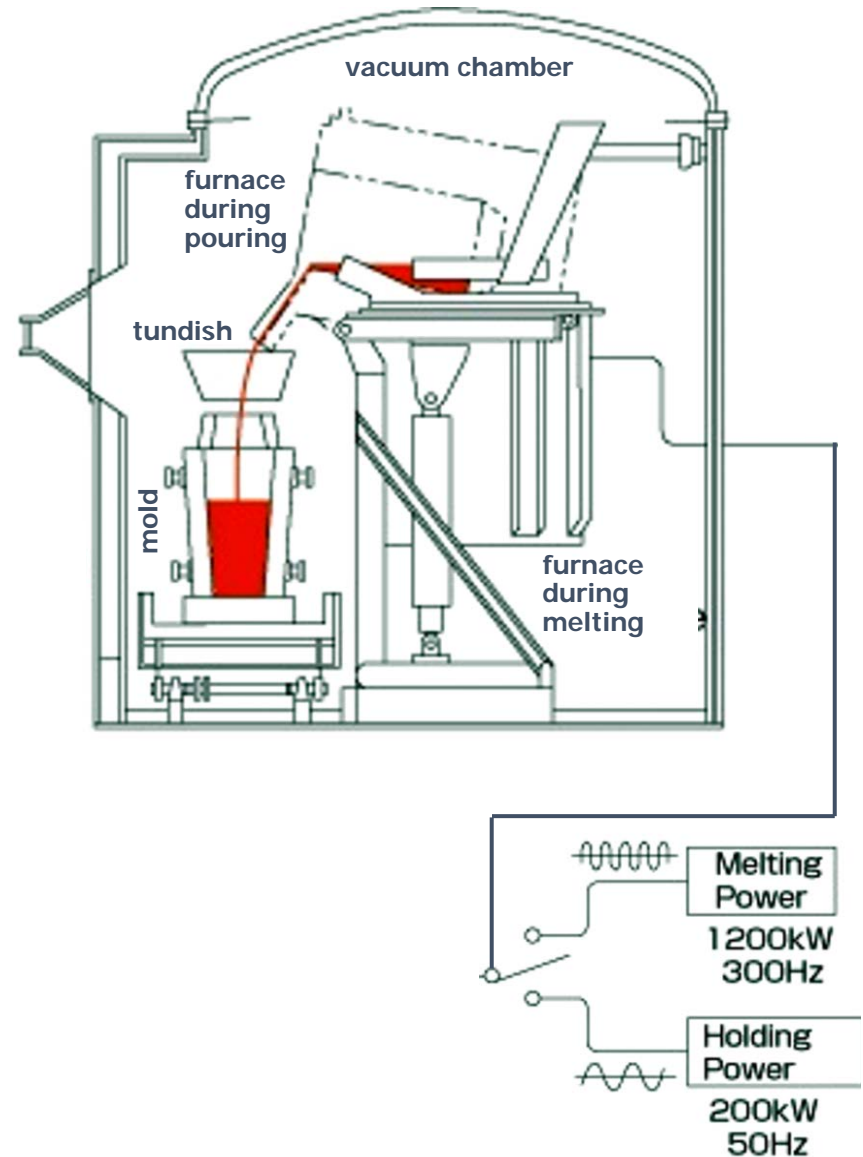
VIM - The Vacuum Induction Melting process involves the melting of metals by means of electromagnetic induction while under vacuum.

Selected material containing few impurities and comparable in chemical composition to the alloy-grade melt is charged into a furnace.

The furnace, consisting of a refractory lining, or "crucible", inside a water-cooled induction coil, is encapsulated in a large vacuum chamber containing sealed hoppers strategically located for adding the required alloys.

The furnace assembly is completely enclosed by a fabricated steel, water-cooled furnace chamber that is evacuated by a series of vacuum pumps so that the charge may be melted down, refined and poured into molds under vacuum or inert gas.

vacuum chamber

furnace during pouring

tundish

mold

furnace during melting

Melting Power
1200kW
300Hz

Holding Power
200kW
50Hz

http://www.sinfo-t.jp/eng/product_info/elec_mecha/no09.html

VAR - In the Vacuum Arc Remelting furnace, the DC electric current is passed through the steel electrode.

The electric arc that is created is similar to a welding arc and produces the heat necessary for remelting of the electrode. The steel gradually melts drop-by-drop in the vacuum-sealed chamber.

Vacuum arc remelting further removes lingering inclusions to provide superior steel cleanliness and further remove gases such as oxygen, nitrogen and hydrogen. Controlling the rate at which these droplets form and solidify ensures a consistency of chemistry and microstructure throughout the entire ingot. This in turn makes the steel more resistant to fracture or fatigue.

http://www.cartech.com/uploadedFiles/Products/Product_Literature/PDF_Files/Whitepaper_PremiumMeltingCarpenterTech.pdf
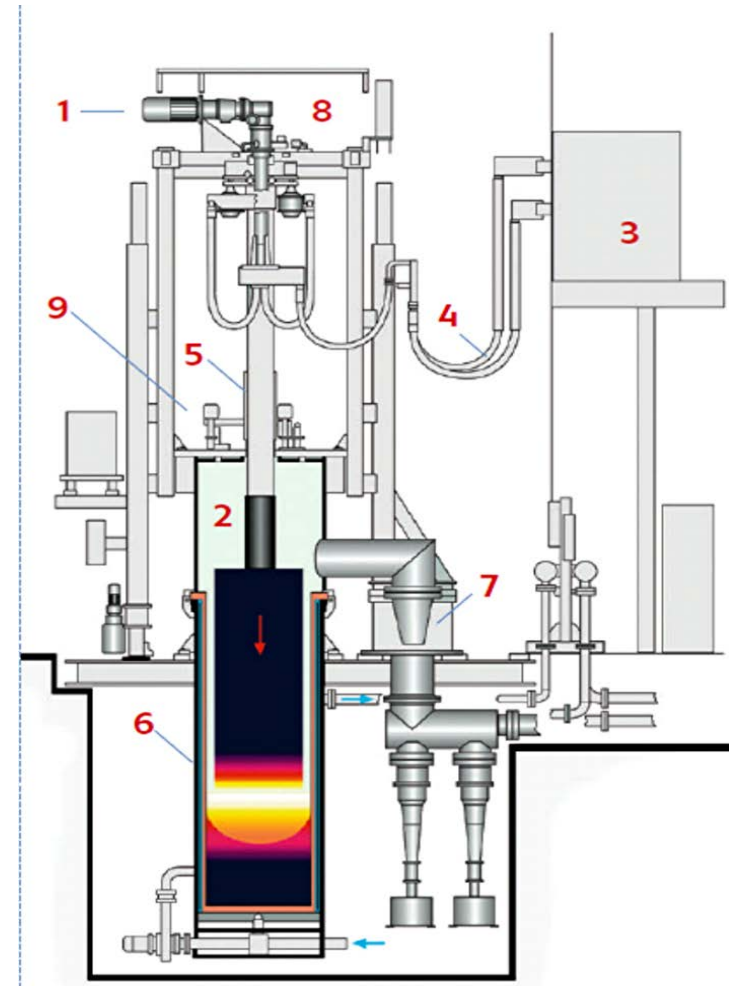
1 Electrode feed drive system   2 Furnace chamber
3 Melting power supply   4 Busbars/cables
5 Electrode ram   6 Water jacket with crucible
7 Vacuum suction port   8 X-Y adjustment
9 Load cell system

Ceramic materials for bearings

Ceramics, for spheres only, have been introduced for high temperature and high speed applications. The following table shows a comparison between materials:

	HRC (20°)	Max T (°C)	ρ kg/dm^3	E MPa	ν /	α (°C^{-1})
M50	64	320	7.6	190000	0.28	$12.3*10^{-6}$
Silicon nitride	78	1200	3.2	310000	0.26	$2.9*10^{-6}$

The reasons for using ceramic materials for balls are explained in the following slides.

Hybrid bearings have rings of bearing steel and rolling elements of bearing grade silicon nitride (Si3N4). In addition to being excellent electric insulators, hybrid bearings have a higher speed capability and will provide longer service life than all-steel bearings in most applications.

The very good electrical insulating property is one of the essential features of the silicon nitride. This protects the rings from electric current damage and so-called washboarding, and thus increases bearing service life.

The density of silicon nitride is only 40% of the density of bearing steel. Thus the rolling elements weigh less and have lower inertia. This means less cage stresses during rapid starts and stops and also significantly lower friction at high speeds.

Lower friction means cooler running and longer lubricant service life. Hybrid bearings are thus suitable for high rotational speeds.

year2009, from the SKF website:
http://www.skf.com/portal/skf/home/products?lang=en&maincatalogue=1&newlink=1_23_1

Under insufficient lubrication conditions there is no smearing between silicon nitride and steel. This enables hybrid bearings to last much longer in applications operating under severe dynamic conditions or lubrication conditions with low operating viscosity.

Silicon nitride has a higher hardness and higher modulus of elasticity than steel, resulting in increased bearing stiffness and longer bearing service life in contaminated environments.

Silicon nitride rolling elements have a lower thermal expansion than steel rolling elements of similar size. This means less sensitivity to temperature gradients within the bearing and more accurate preload control.

However, when designing bearing arrangements for very low temperature and as to estimate reductions in bearing clearance of hybrid bearings *a particular care must be exercised ..., the manufacturer suggests to contact their application engineering service.*

from the mentioned SKF website, 2009